

Exact final state integrals for strong field QED

Victor Dinu

Department of Physics, University of Bucharest, P. O. Box MG-11, Măgurele 077125, Romania

This paper introduces the exact, analytic integration of all final state variables for the process of nonlinear Compton scattering in an intense plane wave laser pulse, improving upon a previously slow and challenging numerical approach. Computationally simple and insightful formulae are derived for the total scattering probability and mean energy-momentum of the emitted radiation. The general form of the effective mass appears explicitly. We consider several limiting cases, and present a quantum correction to Larmor's formula. Numerical results are plotted and analysed in detail.

a. Introduction: The recent and predicted progress in laser technology leading to very high peak intensities justify the need for a better understanding of so-called nonlinear QED, describing phenomena occurring in fields so strong that their effects cannot be treated perturbatively.

Unfortunately, the complexity of the processes inside these ultra-intense laser beams has meant that several simplifications have had to be used to make practical computations feasible. The laser beam is usually supposed to be in a coherent state, which can be well approximated by a classical field. Due to the relatively small frequencies, unless massive particles of very high Lorentz factor are involved, quantum effects are small, so a fully classical description may often be justified. For instance, in discussing the scattering of an electron in a laser beam, one may consider Thompson scattering instead of its quantum counterpart, nonlinear Compton scattering (NLCS) [1]. The classical approximation allows for a realistic description of the laser field and the inclusion of radiation reaction (RR) [2], but is unable to describe important quantum effects, such as nonperturbative pair creation from vacuum [3], the trident process [4], or vacuum birefringence [5].

A treatment of these processes in the framework of nonlinear QED, even in a semiclassical approach, has not yet been performed without further approximations, such as replacing the laser field by an idealized plane wave, thus allowing for analytical (Volkov) solutions to the Dirac equation. This disregards the strong spatial focusing of the beam needed to attain high intensities. In addition, for a long time, results were restricted to infinite, monochromatic plane waves, or even, giving up periodicity, to a crossed field model [6, 7]. Only recently, the more realistic short pulse plane waves came into use [8–10].

In [8, 11, 12], the photonic and electronic distributions resulting from NLCS were described in detail for some model pulses. In principle, by integrating these distributions, the total probability and expectation values, such as for the emitted radiation's energy-momentum, can be obtained. However, previous papers did never plot these quantities, because of the great numerical challenge posed by this task. By a change in integration order and a different regularization, allowing for all final state integrals to be performed analytically, we obtain formulae

that are not only very easy to compute, but offer a new understanding of the scattering mechanism, the effective mass's role, the time coherence of the process and its relation to the classicality parameter. An extensive numerical exploration of the results, their dependence on the various parameters, and their limits, now becomes possible. The method we develop is quite general and shall be applied to other strong field QED processes in a future paper.

b. Preliminaries: For our starting point, notations and conventions, we refer the reader to [13]. In short, $p = mv$ and k' are the initial electron and final photon four-momenta. We opt for natural units, so $c = \hbar = 1$. Define $k = \omega n$, where $n^2 = 0$ and ω is some characteristic frequency of the wave. Let $\phi = k \cdot x = \omega x^-$ be an invariant *lightfront* coordinate, used to describe the plane wave pulse by the four-potential $A = \frac{m}{e} a_0 f(\phi)$. By transversality, $k \cdot A = 0$. We choose $n = (1, \mathbf{e}_3)$, $f_0 = f_3 = 0$, and use lightfront notations such as $p^\pm = p^0 \pm p^3$, $\mathbf{p}^\perp = \mathbf{p} - p^3 \mathbf{n}$. The final results for probability/momentum will prove to be manifestly Lorentz invariant/covariant. While working with $f(\phi)$, only the gauge changes keeping A ϕ -only dependent are allowed. But the end results can be expressed in terms of the classical velocity, so they are gauge invariant. For a long pulse, one may choose ω the carrier frequency and the peak value of the envelope of $f'(\phi)$ equal to one. To compare very short pulses one may prefer to fix ω and a_0 so that the pulse's ϕ range is of order 2π and $-\int d\phi f'^2(\phi) = 1$. Whatever our choice, a_0 should offer a reliable description of the peak intensity, so $\left| f'(\phi)^2 \right|_{\max} \sim 1$.

c. Classical motion: Let $\pi = mu$ be the kinetic momentum of a classical electron moving in this plane wave field, where

$$u(\phi) = v - a_0 f(\phi) + \frac{2a_0 f(\phi) \cdot v - a_0^2 f^2(\phi)}{2k \cdot v} k. \quad (1)$$

If we set $f(-\infty) = 0$, then $v = u(-\infty)$ is indeed the velocity of the particle before meeting the wave. As opposed to unipolar pulses that permanently accelerate the particle [13], for the usual whole-cycle pulses, $f(\infty) = 0$ and $u(\infty) = u(-\infty)$, as long as RR is neglected.

d. Scattering probability: In the Furry picture, the total NLCS probability, averaged over the initial electron's spin and summed over all possible spin/momentum

states of the final particles, is:

$$P = \frac{-\alpha m^2}{4\pi^2 \omega^2 p^-} \int_0^{p^-} \frac{dk'^-}{k'^- (p^- - k'^-)} \int_{\mathbb{R}^2} d\mathbf{k}'^\perp \times \int_{\mathbb{R}^2} d\phi d\phi' \left[1 - a_0^2 g\left(\frac{k'^-}{p^-}\right) \theta^2 \langle f' \rangle^2 \right] e^{\frac{ik' \cdot \langle \pi \rangle \theta}{\omega(p^- - k'^-)}}, \quad (2)$$

where $\theta = \phi' - \phi$, $g(\zeta) = \frac{1}{2} + \frac{\zeta^2}{4(1-\zeta)}$ and we denoted the moving average of a function F by $\langle F \rangle = \theta^{-1} \int_\phi^{\phi'} F(\xi) d\xi$. The formal expression (2) was obtained from formula C1 in [13], as follows. Instead of the expressions C3, we used the unregularized integrals $B_\nu = \int_{\mathbb{R}} \tilde{f}_\nu e^{-i\Phi} d\phi$, with $\tilde{f}_\nu \in (1, f_1, f_2, \mathbf{f}^2)$. Explication of all B_ν in the quadratic form C2 led to the inner double integral in (2), by writing $f(\phi') - f(\phi)$ as $\langle f' \rangle \theta$. Then, the s and \bar{p} integrals were performed, eliminating the four dimensional delta function and imposing the lightfront conservation laws $\bar{p}^\nu = p^\nu - k^\nu$, $\nu \in \{1, 2, -\}$. In the exponent the average of the classical momentum $\langle \pi \rangle$ was identified. A change of variable from k^3 to k^- led to the final result. See also [8–10]. If we want to compute them first, all B_ν in the generic case, or at least B_0 , need to be regulated, damping the oscillations of the integrand with a convergence factor such as $e^{-\varepsilon \phi^2}$, $\varepsilon \searrow 0$, that can be discarded after a partial integration restricts B_ν to the length of the pulse [8, 13].

At first glance, in writing (2) we have added to the numerical complexity, constructing a double integral out of simple ones. But, in fact, by a change of quadrature order, the analytical integration over \mathbf{k}'^\perp , and k'^- leaves us with only two easy integrals, instead of the initial four. In addition, we get rid of the rapid oscillations encountered when computing B_ν . Expressing $k' \cdot \langle \pi \rangle$ in lightfront coordinates, we notice the integral over \mathbf{k}'^\perp is Gaussian, if regulated by replacing in the exponent the factor θ by $\theta + i\varepsilon$, then taking $\varepsilon \searrow 0$. The previous damping factor is now superfluous. Introducing the invariant number $b_0 = \frac{2k \cdot v}{m}$, the result is

$$P = \frac{-i\alpha}{\pi b_0} \int_{\mathbb{R}^2} d\phi d\phi' \int_0^1 d\zeta \frac{1 - a_0^2 g(\zeta) \langle f' \rangle^2 \theta^2}{\theta + i\varepsilon} e^{\frac{i\zeta \mu \theta}{(1-\zeta)b_0}}, \quad (3)$$

where

$$\mu = 1 + a_0^2 \left(\langle f \rangle^2 - \langle f^2 \rangle \right) \geq 1. \quad (4)$$

We recognize the effective mass $M = \sqrt{\langle \pi \rangle^2}$, first introduced by Kibble, that appears in the Volkov propagator [14] and the Wigner function [15, 16]:

$$\mu = \langle u \rangle^2 = \frac{M^2}{m^2}. \quad (5)$$

A Lorentz and gauge invariant, M depends on the averaging interval. For a whole-cycle finite pulse, the mass shift $M - m$ vanishes when $\theta \rightarrow \infty$. We now use the

relation $(\theta + i\varepsilon)^{-1} = p \cdot v \cdot \theta^{-1} - i\pi \delta(\theta)$ and the fact that μ is an even function of θ , so the result is indeed real. Changing variables from ϕ, ϕ' to θ and $\sigma = \frac{\phi + \phi'}{2}$, and noticing that $\pi = \int_{\mathbb{R}} dx \frac{\sin x}{x}$, we get

$$P = -\frac{2\alpha}{\pi b_0} \int_{\mathbb{R}} d\sigma \int_0^\infty d\theta \int_0^1 d\zeta \times \left[\frac{\partial \ln \mu}{\partial \theta} + a_0^2 \langle f' \rangle^2 \theta g(\zeta) \right] \sin \frac{\zeta \mu \theta}{(1-\zeta)b_0}. \quad (6)$$

A new analytical integration leads to:

$$P = -\frac{2\alpha}{\pi b_0} \int_{\mathbb{R}} d\sigma \int_0^\infty d\theta \times \left[\frac{\partial \ln \mu}{\partial \theta} \mathcal{J}_1\left(\frac{\mu\theta}{b_0}\right) + a_0^2 \langle f' \rangle^2 \theta \mathcal{J}_2\left(\frac{\mu\theta}{b_0}\right) \right], \quad (7)$$

where, in terms of trigonometric integrals,

$$\begin{aligned} \mathcal{J}_1(x) &= -xA'(x), \quad \mathcal{J}_2(x) = \frac{1}{8} [2 + x - x^2 A(x)], \\ A(x) &= \sin x \operatorname{ci}(x) - \cos x \operatorname{si}(x), \\ A'(x) &= \cos x \operatorname{ci}(x) + \sin x \operatorname{si}(x). \end{aligned}$$

Notice that the Lorentz invariant (7) depends on b_0 , and 4-products of the values of the function $a_0 f$, but not on $a_0 f \cdot p$. Interestingly, we can rewrite the probability in terms of the classical velocity (1) as function of the proper time, eliminating all reference to the driving field and proving gauge invariance. Could the result be generalized to an arbitrary, not necessarily plane, wave? It is hard to answer, because of the many very different trajectories allowed inside a general field. The attractiveness of a plane wave derives from the simplicity of the law of motion it entails. The electron's motion always looks the same, regardless of the initial position. A quantum computation for a general field would require the use of a wavepacket with some initial average position and momentum that only in the limit relates to a particular classical motion.

e. Radiated energy-momentum: The same procedure can be applied to compute the expectation value of the emitted photon's momentum,

$$\begin{aligned} \langle k'^\nu \rangle &= -\frac{\alpha m^2}{4\pi^2 \omega^2 p^-} \int_0^{p^-} \frac{dk'^-}{k'^- (p^- - k'^-)} \int_{\mathbb{R}^2} d\mathbf{k}'^\perp k'^\nu \\ &\times \int_{\mathbb{R}^2} d\phi d\phi' e^{\frac{ik' \cdot \langle \pi \rangle \theta}{\omega(p^- - k'^-)}} \left[1 - a_0^2 \langle f' \rangle^2 \theta^2 g\left(\frac{k'^-}{p^-}\right) \right]. \end{aligned} \quad (8)$$

Following the same method as for the probability, we are left with the manifestly covariant double integral

$$\langle k'^\nu \rangle = \frac{2\alpha}{\pi} \int_{\mathbb{R}} d\sigma \int_0^\infty d\theta (F \langle \pi^\nu \rangle + G k^\nu), \quad (9)$$

where

$$F = \frac{\mathcal{J}_3\left(\frac{\mu\theta}{b_0}\right) - \mathcal{J}_3\left(\frac{\theta}{b_0}\right)}{b_0\theta} - a_0^2 \langle f' \rangle^2 \frac{\theta}{b_0} \mathcal{J}_4\left(\frac{\mu\theta}{b_0}\right), \quad (10)$$

$$G = \frac{1}{b_0^2} \left(\frac{2-\mu}{\mu} \frac{\partial \mu}{\partial \theta} - 2 \frac{\mu-1}{\theta} \right) \mathcal{J}_3\left(\frac{\mu\theta}{b_0}\right) - \frac{a_0^2}{b_0} \langle f' \rangle^2 \mathcal{J}_5\left(\frac{\mu\theta}{b_0}\right) \quad (11)$$

and the new functions used are

$$\begin{aligned} \mathcal{J}_3(x) &= \frac{x^2}{2} A(x) - x A'(x) - \frac{x}{2}, \\ \mathcal{J}_4(x) &= \frac{1}{24} [(6x - x^3) A(x)]' + \frac{x}{12}, \\ \mathcal{J}_5(x) &= \frac{1}{24} [(x^4 - 6x^2) A(x)]' - \frac{x^2}{8} + \frac{1}{3}. \end{aligned}$$

Notice that $\langle k'' \rangle$ was computed with a distribution normalized not to unity, but to P . Therefore it is not the average value of the momentum of *one* photon, assuming an emission has taken place, but the expected outcome per incident electron, counting both NLCS and elastic scattering events. To compute the former, conditional probabilities are needed. This amounts to dividing the expectation value by P . The standard deviation of k'' or any of its higher moments can similarly be computed.

f. Periodic and adiabatic limits Even though derived for a pulse, our formulae can provide the emission probability and radiated energy-momentum per cycle in the case of an infinite, periodic plane wave, described by $\tilde{f}(\phi) = \tilde{f}(\phi + T)$. They can be obtained by truncating the pulse to a finite number of cycles N , and considering the quickly reached $N \rightarrow \infty$ limit of P/N and $\langle k'' \rangle / N$. The results, that we shall denote by $\tilde{P}(a_0)$ and $\langle \tilde{k}'' \rangle(a_0)$, are given by (7) and (9) with the σ integral restricted to one period. A circularly polarized monochromatic wave $\tilde{f}(\phi) = (0, \cos \phi, \sin \phi, 0)$ provides a simple example, as $\mu = 1 + a_0^2 (1 - \text{sinc}^2 \frac{\theta}{2})$ is independent of σ , so $\int d\sigma \rightarrow 2\pi$. Consider now the modulated wave,

$$f(\phi) = g\left(\frac{\phi}{\tau}\right) \tilde{f}(\phi), \quad (12)$$

where $\tilde{f}(\phi)$ is a periodic function, e.g. monochromatic, the envelope $g(x)$ is a smooth function vanishing at infinity and τ controls the pulse length. Provided $\tau \gg T$, (7) and (9) are practically proportional to τ , being well approximated by

$$P \simeq \frac{\tau}{T} \int_{\mathbb{R}} dx \tilde{P}[a_0 g(x)], \quad (13)$$

$$\langle k'' \rangle \simeq \frac{\tau}{T} \int_{\mathbb{R}} dx \langle \tilde{k}'' \rangle [a_0 g(x)]. \quad (14)$$

Of particular interest are the limiting cases of small a_0 or b_0 . With today's technology, ω is around the order of

$1 - 10^4$ eV and only for the optical range a large a_0 is possible. If, for instance, $\omega = 3$ eV, an electron energy of at least 20 GeV is needed for b_0 to reach unity.

g. Perturbative limit The results can be expressed as integrals containing the field's Fourier transform and the Klein-Nishima probability of linear Compton [13]. However, to emphasize the role of b_0 , we prefer to work with a quadratic function related to the potential's auto-correlation,

$$\mathcal{E}(\theta) = -a_0^2 \int_{\mathbb{R}} d\sigma \langle f' \rangle^2. \quad (15)$$

The weak field limits ($a_0 \ll 1$) of (7) and (9) are:

$$P_p = \frac{2\alpha}{\pi} \int_0^\infty d\theta \mathcal{P}\left(\frac{\theta}{b_0}\right) \mathcal{E}(\theta), \quad (16)$$

$$\langle k'' \rangle_p = \frac{2\alpha}{\pi} \int_0^\infty d\theta \left[p'' \mathcal{F}\left(\frac{\theta}{b_0}\right) + k'' \mathcal{G}\left(\frac{\theta}{b_0}\right) \right] \mathcal{E}(\theta), \quad (17)$$

where \mathcal{P} , \mathcal{F} , and \mathcal{G} are the universal, positive functions,

$$\begin{aligned} \mathcal{P}(x) &= x^2 \int_x^\infty \frac{y-2x}{y^3} \mathcal{J}_1(y) dy + x \mathcal{J}_2(x), \\ \mathcal{F}(x) &= x^2 \int_x^\infty \frac{y-2x}{y^3} \mathcal{J}_3(y) dy + x \mathcal{J}_4(x), \\ \mathcal{G}(x) &= x^2 \int_x^\infty \frac{4x-3y}{y^3} \mathcal{J}_3(y) dy + \mathcal{J}_5(x). \end{aligned}$$

Since $\mathcal{P}(x)$ is increasing for $x > 0$, 16 decreases with b_0 , having the classical upper bound

$$P_{p, cl} = \frac{2\alpha}{3\pi} \int_0^\infty d\theta \mathcal{E}(\theta).$$

h. Classical limit: This is expected when $b_0 \ll 1$, since b_0 is proportional to \hbar , a fact obscured by the use of natural units. That is, the laser photon energies are much smaller than m in the electron's rest frame. Now the major contribution to the integral (9) comes from small θ . By Taylor expansions, such as

$$\mu = 1 + a_0^2 \left[\frac{-f'(\sigma)^2}{12} \theta^2 + \mathcal{O}(\theta^4) \right], \quad (18)$$

one obtains the approximation

$$\langle k'' \rangle \simeq -\frac{\alpha}{3} b_0 a_0^2 \int_{\mathbb{R}} d\sigma \pi''(\sigma) f'(\sigma)^2 \mathcal{C} \left[-\frac{b_0^2 a_0^2 f'(\sigma)^2}{12} \right], \quad (19)$$

where

$$\mathcal{C}(x) = \frac{1}{\pi} \int_0^\infty [6\mathcal{J}_4(y + xy^3) - \mathcal{J}_3(y + xy^3)] y dy. \quad (20)$$

No classical equivalent is found for the second term in the integrand of (9), negligible in this limit. An equivalent form of (19) can be written by expressing everything

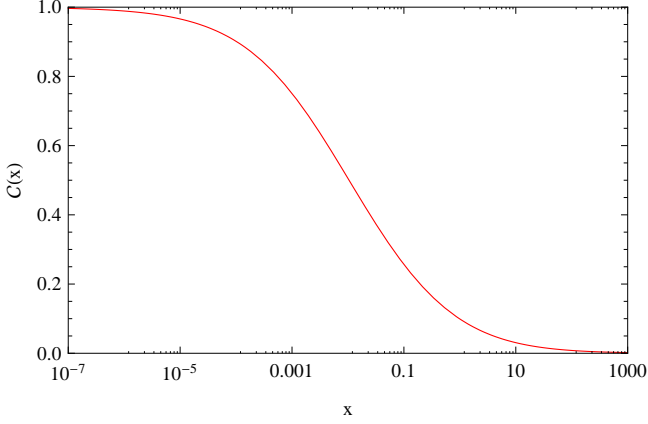


FIG. 1: (color online) The function describing the strong field correction to Larmor's formula

in terms of a classical particle's velocity as function of proper time,

$$\langle k'^\nu \rangle \simeq -\frac{1}{6} \frac{e^2}{\pi} \int_{\mathbb{R}} d\tau u^\nu(\tau) \dot{u}(\tau)^2 \mathcal{C} \left[-\frac{\dot{u}(\tau)^2}{3m^2} \right]. \quad (21)$$

When not only b_0 , but also $b_0 a_0$ is very small, equation (21) further reduces to:

$$\langle k'^\nu \rangle_{cl} = -\frac{1}{6} \frac{e^2}{\pi} \int_{\mathbb{R}} d\tau u^\nu(\tau) \dot{u}(\tau)^2. \quad (22)$$

The same result arises directly from classical electrodynamics, if one neglects radiation reaction. For $\nu = 0$, (22) is just the time integrated Larmor's formula.

The function (20) is decreasing for $x > 0$. As shown in Fig. 1, it departs very quickly from its upper bound $\mathcal{C}[0] = 1$. The deviation is noticeable even for $x = 10^{-5}$. It follows that a small b_0 doesn't necessarily make classical Thompson scattering a good model. For strong fields, much less power is radiated than Larmor predicts. In CED, the spectral and angular distribution is also a double integral, but an interesting cancelling of interference terms leaves a single one after the frequency is integrated away. The transfer of energy and momentum to the field is well defined at each moment in time, there are no quantum uncertainties. Interestingly, this form of decoherence is also shown by the better approximation (21), that looks misleadingly classical, though the argument of the correction \mathcal{C} is in fact proportional to \hbar^2 . Heuristically, b_0 is a coherence lightfront time θ scale. When small enough, it allows for a time-incoherent model of emission, but at high intensities the mass shift implied by (18) cannot be neglected in this coherence interval, hence the aforementioned correction. This happens when the peak electric field in the electron rest frame approaches the Schwinger critical value m^2/e . Formula (21) could provide a general improvement to Larmor's, valid in an arbitrary driving field, whose frequencies in the rest frame of the electron

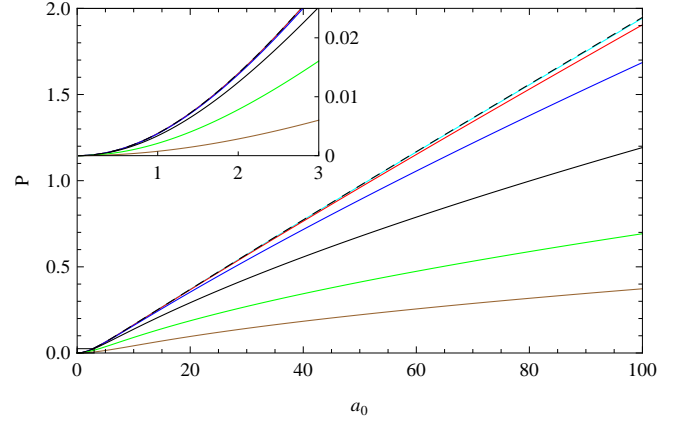


FIG. 2: (color online) The NLCS probability (7) is plotted as function of a_0 , for the pulse (24) and $b_0 = 10^p$, $p = -4, -3, \dots, 1$. The dashed line is the classical limit (23). The inset details the perturbative region of small a_0 .

are similarly low compared to m , so the emission can be viewed as incoherent in time, hence the product of the classical motion of a charged particle. This should not be confused to the second term in the radiated energy's expansion in powers of \hbar , at fixed a_0 , that is non-local in time, as discussed in [17, 18]. As for the total scattering probability, by an asymptotic expansion of the functions $\mathcal{J}_i(x)$ one gets the limit

$$P_{cl} = \frac{2\alpha}{\pi} a_0^2 \int_0^\infty \frac{d\theta}{\theta^2} \int_{\mathbb{R}} d\sigma \frac{\langle f^2 \rangle - \langle f \rangle^2 - \frac{1}{2} \langle f' \rangle^2 \theta^2}{1 + a_0^2 (\langle f \rangle^2 - \langle f^2 \rangle)}. \quad (23)$$

In this case no decoherence is observed, as photon emission probability is not a classical concept.

i. Numerical results: We start illustrating our results using a one-cycle, linearly polarized pulse, characterized by a Gaussian potential:

$$f^\mu(\phi) = \sqrt[4]{\frac{2}{\pi}} \exp(-x^2) \delta_{\mu 1}. \quad (24)$$

The total NLCS probability is shown in Fig.2. The quadratic increase from the perturbative region, shown in detail in the upper left corner, quickly slows down as a_0 grows past unity. The higher the parameter b_0 , the lower P is. In general, (7) boundlessly grows with the length/intensity of the pulse. Even for one as short as (24) and the experimentally attainable $a_0 = 100$, the result can easily surpass unity. In [19], this possibility was noticed, interpreted as a sign that multiphoton emission cannot then be neglected, and a re-normalization of the whole series of n-photon NLCS probabilities was suggested. Moreover, for a unipolar pulse, (7) shows the logarithmic IR divergence typical of Bremsstrahlung [13, 20]. These problems can be dealt with by including a one loop self-energy diagram, that adds nothing to (9), but does contribute to the expectation value of the final electron's momentum, even in the whole-cycle case [21].

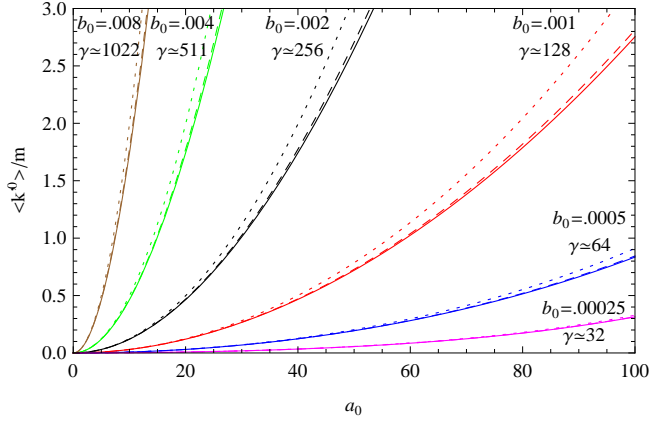


FIG. 3: (color online) The expectation value of $\langle k^0 \rangle$, as a multiple of the electron rest energy, plotted as function of a_0 , for the pulse (24). The dotted line is the Thompson limit (22), while the dashed one is the better approximation (21).

For the general theory of the cancellation between real and virtual photon IR divergences, see [22].

To plot formula (9), we need more than just the invariants a_0, b_0 . The frequency of any available laser that can reach the nonlinear regime $a_0 \gtrsim 1$ is around the optical range. Let's assume $\omega = 1$ eV. It remains to know the incidence, that we choose head-on. While experimentally difficult, this gives the largest b_0 for a given pulse and electron beam. In Fig. 3 a comparison is drawn between the expectation value of the radiated energy and its two incoherent approximations. Both (22) and (21) overestimate (9), but the latter is a much closer match.

Let us now consider a modulated harmonic wave,

$$f(\phi) = g\left(\frac{\phi}{\tau}\right) (0, \cos \xi \sin(\phi - \phi_0), \sin \xi \cos(\phi - \phi_0), 0), \quad (25)$$

where ξ describes the polarization state, ϕ_0 is known as carrier-envelope phase (CEP) and τ controls the pulse length. We present computations for the symmetric, Gaussian envelope $g(x) = e^{-x^2}$. For the carrier-envelope model to make sense, we assume τ is larger than, say, π . Fig. 4, shows contour plots of the total probability (7) as function of pulse peak potential/length, for linear polarization and various values of the nonclassicality parameter b_0 . Again, we find that in experimentally realistic conditions, our result can easily surpass unity, signalling the need for taking into account higher order Feynman diagrams. We are interested in the region where P stays well below unity, so the model can be given credit. This region grows with b_0 , once it gets close to unity. The influence of the polarization state and the convergence towards the adiabatic limit (13), as the pulse length increases, are shown in Fig. 5. The CEP ϕ_0 has a very small impact on P for this smooth potential.

In order to study (9), we now choose an optical fre-

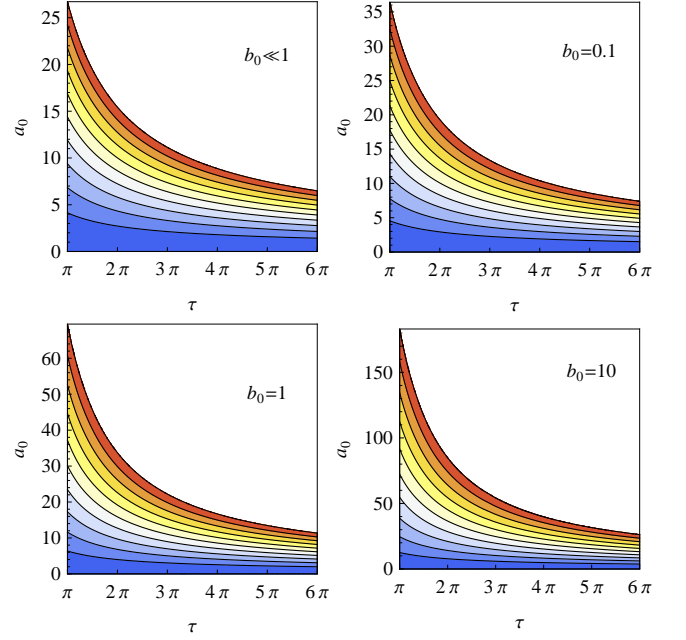


FIG. 4: (color online) Contour plot of the NLCS probability (7), in terms of the duration/strength of the pulse (25), for linear polarization and $\phi_0 = 0$. The contours correspond to $P = 0.1, 0.2, \dots, 1$.

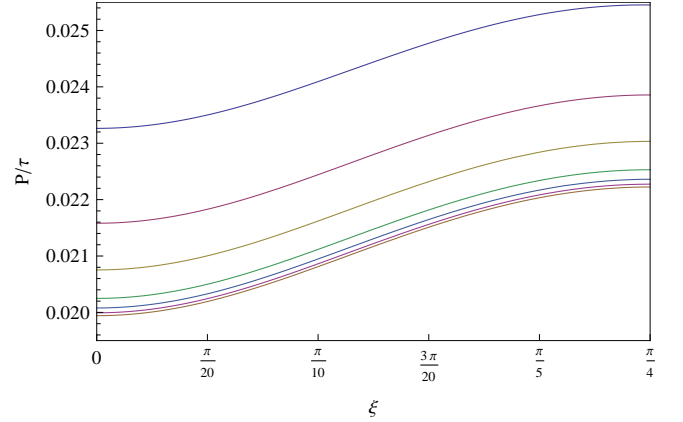


FIG. 5: (color online) The probability (7) divided by the length of the pulse (25), as function of polarization state, for $a_0 = 5$, $b_0 = 1$ and $\phi_0 = 0$. The curves correspond, in decreasing order, to $\tau/\pi = 1, 2, 4, 10, 20, 40, 100$.

quency of 3 eV, and specify the initial electron momentum, setting its Lorentz factor v^0 and polar angles θ_p and ϕ_p . We have already looked at the energy $\langle k^0 \rangle$ for a one-cycle pulse, so we consider a longer one. In Fig. 6 a plot of the radiated energy's dependence on the initial electron energy is shown for the pulse (25) with $\tau = 3\pi$, linear polarization and $a_0 = 10$. In the classical regime, after v^0 becomes much greater than a_0 , the growth is quadratic, but at even higher energies quantum effects

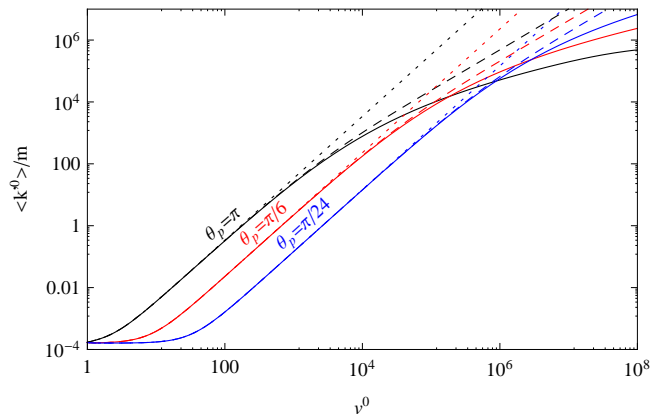


FIG. 6: (color online) A plot of the expectation value $\langle k'^0 \rangle$ versus the initial electron's Lorentz factor for the pulse (25) with $\tau = 3\pi$, $\xi = \phi_0 = 0$ and $a_0 = 10$. The incidence angles are $\theta_p = \pi$, $\frac{\pi}{6}$, $\frac{\pi}{24}$ and $\phi_p = 0$. The head-on result is much larger at low energies, surpassed by the others at very high ones. The dotted/dashed lines are the approximations (22) and (21).

slow it down. For a while, it is well described by the local in time, incoherent approximation (21). Then, as b_0 goes past unity, we reach a highly nonlocal quantum radiation regime. It is interesting to notice that, at very high energies, the emission becomes stronger for lower incidence angles θ_p than for higher ones, because the corresponding smaller b_0 implies weaker quantum effects. Fig. 7 shows the increase of $\langle k'^0 \rangle$ as the polarization is changed from linear towards circular. The influence of ϕ_p on (9) is due to the $f(\phi) \cdot v$ term in (1). For the example considered in Fig. 6, both this dependence and the one on the CEP ϕ_0 are extremely weak. They can be noticeable for a very short pulse and small b_0 , as seen from the example in Fig. 8. As to the vector $\langle \mathbf{k}' \rangle$, for large v^0 , it practically has the direction of \mathbf{v} and the length $\langle k'^0 \rangle$, in the laboratory frame all emission being concentrated inside a very narrow cone. Significant differences arise only at low energies, where quantum effects are, however, small.

j. Conclusions: We have found a way to analytically integrate all final state variables out of the NLCS probability and expectation values. This not only allowed for the first time their detailed numerical exploration, by saving huge computational expense, but also revealed new insights into the structure of scattering processes in strong fields. We shed light on the role of the effective mass and the emission's coherence in time. Simple results were found for the monochromatic, perturbative and classical limits. We derived a strong field correction to Larmor's formula, arising from the mass shift. Computations performed under realistic conditions showed its

usefulness, but also found large values for the probability, even surpassing unity. This suggests multiple scatterings and radiative corrections need to be considered. In a fu-

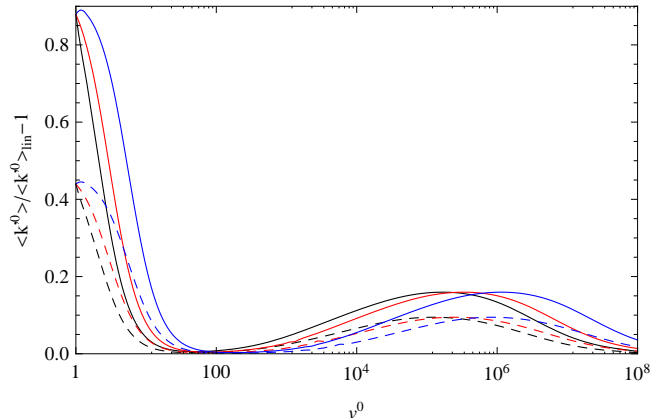


FIG. 7: (color online) The relative increase in the average radiated energy when the polarization is changed from linear to circular ($\xi = \frac{\pi}{4}$, solid line) / elliptic ($\xi = \frac{\pi}{8}$, dashed line). The pulse is (25), $\tau = 3\pi$, $\phi_0 = 0$, $a_0 = 10$, $\phi_p = 0$ and $\theta_p = \pi$, $\frac{\pi}{2}$, $\frac{\pi}{4}$ (growing order at left)

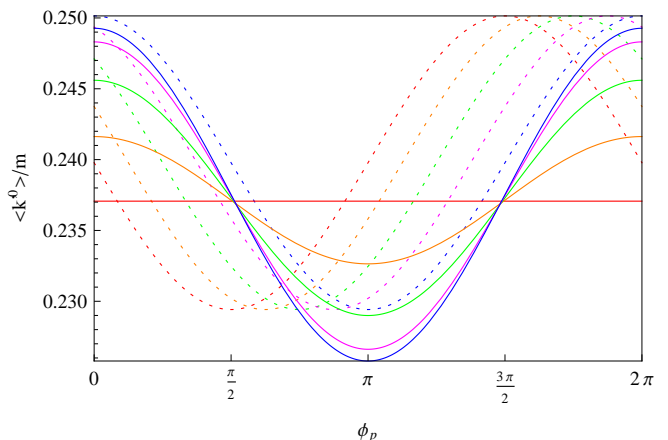


FIG. 8: (color online) The radiated energy's dependence on the angle ϕ_p , for $\theta_p = \frac{\pi}{2}$, $\gamma = 100$ and the pulse (25), with $\tau = \pi$, $a_0 = 20$ and CEP $\phi_0 = 0, \frac{\pi}{8}, \frac{\pi}{4}, \frac{3\pi}{8}, \frac{\pi}{2}$ (growing order at left). Solid/dotted stand for circular/linear polarization.

ture paper, our method will be applied to these, as well as to other strong field processes.

k. Acknowledgements The author thanks V. Florescu, A. Ilderton and G. Torgrimsson for useful discussions, and ESF-RNP-SILMI for support in attending conference FILMITH, Garching 2012

- [3] G.V. Dunne, Eur. Phys. J. D 55, 327 (2009).
- [4] A. Ilderton, Phys. Rev. Lett. 106, 020404 (2011).
- [5] T. Heinzl, B. Liesfeld, K.-U. Amthor, H. Schwöerer, R. Sauerbrey, and A. Wipf, Opt. Commun. 267, 318 (2006).
- [6] A. I. Nikishov, V. I. Ritus, Sov. Phys. JETP 19, 529 (1964).
- [7] N. B. Narozhnyi, A. I. Nikishov, V. I. Ritus, Sov. Phys. JETP 20, 622 (1965).
- [8] M. Boca and V. Florescu, Phys. Rev. A 80, 053403 (2009).
- [9] T. Heinzl, D. Seipt, B. Kämpfer, Phys. Rev. A 81, 022125 (2010).
- [10] D. Seipt, B. Kämpfer, Phys. Rev. A 83, 022101(2011).
- [11] M. Boca, V. Dinu, V. Florescu, Phys. Rev. A 86, 013414 (2012).
- [12] F. Mackenroth, A. DiPiazza, Phys. Rev. A 83, 032106 (2011).
- [13] V. Dinu, T. Heinzl, A. Ilderton, Phys. Rev. D 86, 085037 (2012).
- [14] T. W. B. Kibble, A. Salam, J. Strathdee, Nucl. Phys. B96 (1975) 255.
- [15] F. Hebenstreit, A. Ilderton, M. Marklund, J. Zamanian, Phys. Rev. D83 (2011) 065007.
- [16] C. Harvey, T. Heinzl, A. Ilderton, M. Marklund, arXiv:1203.6077 [hep-ph].
- [17] A. Higuchi and P. J. Walker, Phys. Rev. D 80, 105019 (2009).
- [18] K. Yamamoto, G. Nakamura, Phys. Rev. D 83, 045030 (2011).
- [19] A. Di Piazza, K. Z. Hatsagortsyan, C. H. Keitel, Phys.Rev.Lett.105, 220403 (2010).
- [20] A. Ilderton, G. Torgrimsson, arXiv:1210.6840 [hep-th].
- [21] A. Ilderton, G. Torgrimsson, arXiv:1301.6499 [hep-th].
- [22] D. R. Yennie, S. C. Frautschi, H. Suura, Ann. Phys. 13, 379 (1961).